Engineering Science and Technology, an International Journal 19 (2016) 1742–1752

HOSTED BY

Contents lists available at ScienceDirect

Engineering Science and Technology, an International Journal

journal homepage: www.elsevier.com/locate/jestch

Full Length Article

Improved LVRT for grid connected DFIG using enhanced field oriented control technique with super capacitor as external energy storage system

V.N. Ananth Duggirala [a], V. Nagesh Kumar Gundavarapu [b,*]

[a] Department of EEE, Viswanadha Institute of Technology and Management, Visakhapatnam 531173, India
[b] Department of EEE, GITAM University, Visakhapatnam 530045, Andhra Pradesh, India

ARTICLE INFO

Article history:
Received 19 June 2016
Revised 21 July 2016
Accepted 26 July 2016
Available online 21 August 2016

Keywords:
DFIG
Field oriented control (FOC)
Low voltage fault ride through (LVRT)
Voltage sag
Voltage mitigation

ABSTRACT

During faults, severe inrush current of magnitude 2–5 times reaches DFIG stator and rotor terminals damaging its windings. Many control schemes are developed to limit to these inrush currents to 2 times but face issues like over speeding of generator, dc voltage fluctuations etc. To overcome the issues and limit the current within 2 times for faults, enhanced field oriented control technique (EFOC) was implemented in the Rotor Side Control (RSC) of DFIG converter. This technique can control oscillations in torque, speed and flux components of DFIG during and after faults. New equations and generator converter control schemes are proposed. This converter topology uses a super capacitor energy storage system (SCESS) in parallel to a normal capacitor for additional reactive power support to further to improve performance of DFIG during the faults. The SCESS helps in maintaining nearly constant voltage profile across the dc link capacitor. In EFOC technique, the reference value of rotor flux changes its value of super-synchronous slip speed to a small value of zero during the fault with the injecting rotor current at the rotor slip frequency during normal operation. In this process dc-offset component of flux is controlled for decomposition during faults. The system performance with symmetrical and asymmetrical fault is analyzed using simulation studies.

1. Introduction

The doubly fed induction generator (DFIG) is having many advantages compared to the same class of other generators. It's smaller in size of higher MVA ratings commercially available in the market with low power ratings of converters. It can operate in variable generator speed but with constant frequency, vigorous four quadrant reactive power control and better performance during the different types of faults. But, DFIG is sensitive to external turbulences like voltage swell and sag. If grid voltage decreased suddenly due to any faults, large surge currents reach the rotor terminals and voltage decreases and speed of rotor increases significantly, which makes the DFIG to lose synchronism. Hence, the rotor side converter (RSC) will get damaged due to exceeding voltage or the current rating and speed. Also, huge electromagnetic torque pulsation, rotor speed increases and large flux fluctuations in both stator and rotor windings occur which may reduce gear wheels of the wind turbine-generator lifetime. The DFIG must remain in synchronism during any faults for certain period based on the nation grid code is called low voltage ride through (LVRT).

The LVRT issues with DFIG during different faults and comparative study using different control strategies is available in [1]. The capability of RSC is studied in [2] to control fault current entering into DFIG with desired reactive power compensation to improve the stability during fault. The technique adopted in this paper is, it is studied that the behavior of DFIG when the stator and rotor voltages is dropped to a certain value during fault, how the DFIG wind turbine system maintains synchronization and reaches its pre-fault state. For LVRT improvement, Control strategy based on flux trajectory [3], improved reactive power maintenance [4], DC link current of RSC control so as to smoothen DC voltage fluctuations during grid faults using stored Kinetic Energy [5] are used. Additional energy storage devices are used to get support for additional real and reactive power during faults. The crowbar as passive and active RSC strategy for LVRT improvement and reactive power compensation [6], FFTC scheme with PIR [7] and PI [8] with symmetrical and asymmetrical faults is used. In these papers, instead of the conventional PI controller, PI + Resonant controller is used

* Corresponding author.
E-mail address: drgvnk14@gmail.com (V. Nagesh Kumar Gundavarapu).
Peer review under responsibility of Karabuk University.

http://dx.doi.org/10.1016/j.jestch.2016.07.014
2215-0986/

to improve LVRT issue. Few intelligent control techniques like Genetic Algorithm [9], PSO, ANN, fuzzy, bacterial search etc are also used in control strategies for improving the performance during LVRT. Some external passive elements and active energy sources in coordination with normal capacitor are used for improving stability and better LVRT operation of DFIG during faults. Among external devices, Single phase crowbar [11], Super-capacitor energy storage system [12], Fault Current Limiter (FCL) [13], Superconducting FCL with Magnetic Energy storage devices [14] are becoming famous now days. Using these with sophisticated control strategies, conventional crowbar circuit can be avoided. Otherwise, it will disable DFIG in providing reactive power support to the grid during critical state. From these papers, active energy storage devices help in rapid real and reactive power support for stator and rotor terminals for better stability during any faults.

If a symmetrical fault occurs near grid, the DFIG stator and rotor windings and thereby converters will get damaged due to the inrush currents entering into the DFIG windings. It is due to the surge currents which are almost dc in nature with high magnitude. If this dc offset component of flux or current is controlled, lifetime of DFIG can be improved and also performance during the fault can be made better. Similarly asymmetric faults will produce negative sequence components in flux resulting in high stator currents and large torque and power oscillations. All these must be controlled using a simple control scheme to withstand any type of fault and with any severity for a given time period as per grid codes. Therefore enhanced field oriented control (EFOC) scheme is proposed to overcome all the issues.

A conventional vector control methods in RSC do not afford low magnitude rotor over currents. They activate the crowbar, forcing wind energy system to demand reactive power. With the EFOC, improved diminution in the rotor over currents is made promising by considering the effect of direct axis stator flux ϕ_{ds} aligned with rotating stator flux. Ultra capacitors or sometimes called as super capacitors energy storage systems (SCESS) are recently used [15–23] to improve the LVRT behavior of grid connected DFIG. The SCESS is connected to the dc link between the back to back converters of DFIG. It is used to supply additional real and reactive power to the RSC and GSC to enhance the operation during faults. Normal capacitor with low rating converters with sophisticated ride through algorithms can improve much extent the performance of DFIG during faults, but with external devices, the performance can be much better was improved on the external energy storage devices like SCESS. To the degree that storage technique is concerned, battery storage is an alternative for its cost effectiveness while Super Magnetic Energy Storage system is much expensive and fly-wheel [24], [25] receive large time constant to give better dynamic support to overall wind energy system [9]. The to and fro energy flow directions in BESS is associated with real and reactive flows to the grid. Different control strategies [26–29] are used for fault ride through during symmetrical or asymmetrical faults or harmonic environment for DFIG wind system. Using chopper circuit like Z-source inverter is used for fixed speed induction generator for wind power applications is given in [30] and application and control strategy for super-capacitor energy storage is given in [31] is used for dc-dc voltage boost application. The doubly fed induction motor performance is studied in [32,33] for the applications like pumped storage plant. In [32], voltage sag of types A, B and C are considered and using the control strategy for RSC, the performance is improved. A hybrid electric source of wind and diesel are considered in [34] using computer simulation. A technical review of different MPPT techniques for different generators is studied in [35] and stating the advantages and disadvantages of particular application and rating. A thorough investigation into squirrel-cage induction generator of single stage power converter is described in detail in [36].

This paper describes the LVRT behavior of DFIG during faults without sacrificing dynamic stability and improved operation during and after the faults. For this advanced EFOC technique and support of external energy storage system connected to bidirectional switches to the dc link is useful. The performance of DFIG during faults is improved when compared with conventional control strategies. The external device helps to maintain voltage at the dc link terminal and to get better dynamic stability during any grid disturbances. This paper compares results for DFIG grid connected system without and with SCESS to the DC link during low voltage disturbances at the grid. It also explicates how well a rotor current is controlled with flux oriented demagnetisation mechanism.

The rotor and stator flux variations must be controlled during fault, along with electromagnetic torque, rotor speed and machine currents for effective operation of DFIG. To achieve this, the first step is, a new reference synchronous speed has to be chosen based on change in speed during fault. Second step is, DC offset component of flux must be eliminated, oscillations must be damped and change in magnitude of q axis flux components must be controlled. This methodology is termed as EFOC. The efficacy of EFOC is analyzed for a standard DFIG system for improving voltage and current profile of stator and rotor with stable torque, speed and flux control mechanism.

In the Section 2, the mathematical modelling of RSC for EFOC under steady and transient state is explained. Section 3 describes the design of super-capacitor and its control circuit for dynamic compensation. In Section 4, the MATLAB simulation results when an asymmetrical and symmetrical fault occurs to PCC with 70% decrease in the rated voltage. The conclusion is given in section 5 followed by appendix and references.

2. Mathematical analysis of RSC of DFIG during steady state and transient state

The conventional demagnetization or field oriented control (FOC) schemes against DFIG is adopted in a synchronously rotating frame. It is to assist in decoupled active and reactive power management and to improve the system operation during transients with better dynamic response. The DFIG equivalent circuit [1,2,10,26], the dynamics of vectors is shown in GSC and RSC control schemes in Figs. 1 and 2. The external control loop for GSC derives relation between wind speed and mechanical power is done as per the Table 1.

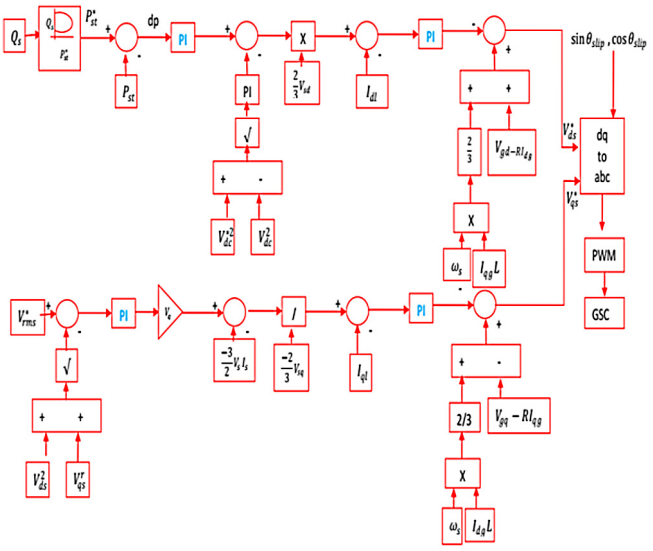

Fig. 1. Block diagram of GSC controller design for Grid connected DFIG.

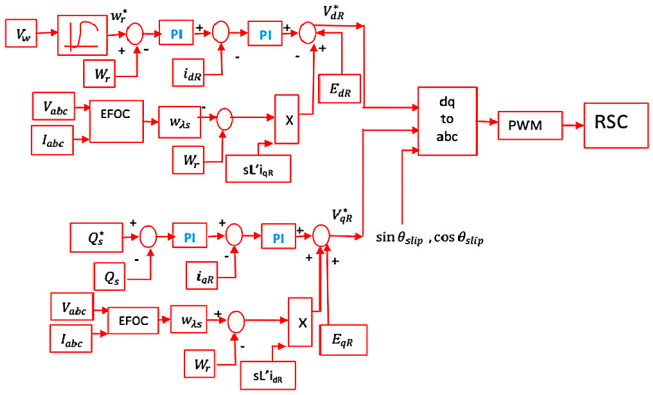

Fig. 2. block diagram of the RSC controller with EFOC technique design for Grid connected DFIG.

Table 1
Lookup table showing the relation of wind speed, rotor speed, mechanical power and output torque for certain speeds.

$V_{wind}(m/s)$	7	8	9	10	11	12	18
w_r (pu)	0.75	0.85	0.95	1.05	1.1	1.2	1.3
P_m (pu)	0.32	0.49	0.69	0.9	1	1.15	1.5
$T_{m=\frac{P_m}{w_r}}$ (pu)	0.48	0.58	0.73	0.85	0.9	0.95	1.15

2.1. 2A. Rotor side converter control during steady state

RSC controller helps in maintaining reactive power demanded by grid (Q_{grid}) also in extracting maximum power from the generator, making the rotor to run at optimal speed. The optimal rotor speed is decided on machine real power and rotor speed characteristic curves as shown in Table 1 for MPPT algorithm. The stator active and reactive power management is possible with the RSC control strategy using i_{qr} and i_{dr} components controlling. The rotor voltage in the stationary reference frame [11,29] is given by

$$V_r^s = V_{0r}^s + R_r i_r^s + \sigma L_r \frac{di_r^s}{dt} - \omega\, i_r^s \tag{1a}$$

where, $\sigma = 1 - \frac{L_{sm}^2}{L_s L_r}$ and ω is the rotor speed, i_r^s is the rotor current in a stationary reference frame, L_s, L_r and L_m are the stator, rotor and mutual inductance parameters in pu (per-unit) or in henry.

$$V_{0r}^s = \frac{L_m}{L_s}\left(\frac{d}{dt} + j\,\omega_s\right)\Phi_s^s \tag{1b}$$

It is the voltage induced in the stator flux with

$$\begin{cases} \Phi_s^s = L_s i_s^s + L_m i_r^s \\ \Phi_r^s = L_r i_r^s + L_m i_s^s \end{cases} \tag{2}$$

The d and q axis rotor voltage Eqs. (1a), (1b), and (2) in the synchronous rotating reference frame are given by

$$\begin{cases} V_{dr} = \frac{d\Phi_{dr}}{dt} - (\omega_s - \omega)\Phi_{qr} + R_r i_{dr} \\ V_{qr} = \frac{d\Phi_{qr}}{dt} + (\omega_s - \omega)\Phi_{dr} + R_r i_{qr} \end{cases} \tag{3}$$

The stator and rotor two axis fluxes are

$$\begin{cases} \Phi_{dr} = (L_{lr} + L_m) i_{dr} + L_m i_{ds} \\ \Phi_{qr} = (L_{lr} + L_m) i_{qr} + L_m i_{qs} \\ \Phi_{ds} = (L_{ls} + L_m) i_{ds} + L_m i_{dr} \\ \Phi_{qs} = (L_{ls} + L_m) i_{qs} + L_m i_{qr} \end{cases} \tag{4}$$

where, $L_r = L_{lr} + L_m$, $L_s = L_{ls} + L_m$, $\omega_r = \omega_s - \omega$

By substituting Eqs. (4) in (3) and by rearranging the terms, then

$$\begin{cases} V_{dr} = \left(R_r + \frac{dL_r'}{dt}\right) i_{dr} - s\omega_s L_r' i_{qr} + \frac{L_m}{L_s} V_{ds} \\ V_{qr} = \left(R_r + \frac{dL_r'}{dt}\right) i_{qr} + s\omega_s L_r' i_{dr} + \frac{L_m}{L_s}(V_{qs} - \omega\Phi_{ds}) \end{cases} \tag{5}$$

From literature, the torque equation can be written as

$$T_e = K_p(\Phi_{qs}\Phi_{dr} - \Phi_{ds}\Phi_{qr}) \tag{6}$$

where ω is rotor speed, $\omega_{\Phi s}$ is speed of stator flux, ω_s is synchronous speed. K_p is a constant of $1.5(n_p{}^* L_m/(L_s L_r - L_m^2)$.

The above Eq. (5) is rewritten in terms of decoupled parameters and is designed for RSC controller as in Eq. (7).

$$\begin{cases} V_{dr} = \sigma L_r \frac{dI_{dr}}{dt} + \omega_s \Phi_{qr} + \frac{L_m}{L_s}(V_{ds} - R_s I_{ds} + \frac{L_s}{L_m}\omega_1 \Phi_{qr}) + R_r i_{dr} \\ V_{qr} = \sigma L_r \frac{dI_{qr}}{dt} - \omega_s \Phi_{dr} - \frac{L_m}{L_s}(R_s I_{qs} - \frac{L_s}{L_m}\omega_1 \Phi_{ds} - V_{qs}) + R_r i_{qr} \end{cases} \tag{7}$$

In general the rotor speed is ω_r and the synchronous speed of stator, ω_s. But this synchronous frequency has to be changed from ω_s to a new synchronous speed value ω_s' as it is represented commonly by ω_1. Under ideal conditions, reference stator d-axis flux Φ_d^* is zero and the q-axis stator flux Φ_q^* is equal to the magnitude of stator flux Φ_s for given back emf and rotor speed.

The flux derivation method helps in considering the DFIG during steady state and transient state operation. The accuracy of system operation during steady state depends on precision of wind speed measurement and action of pitch angle controller, quantity of stator current, voltage, flux and other generator parameters. The precise in determining these parameters, the more real power extraction from generator- turbine set increases. The equations from (5) to (7) are important to indulging the behavior of DFIG during steady state. The accuracy of RSC control scheme depends on control of d and q axis voltages by PWM controller.

2.2. 2B Three phase symmetrical faults

The stator voltage will become zero in value during three phase symmetrical fault with low impedance. This makes the stator flux Φ_s value get reduced to zero magnitude gradually. The flux decay is not rapid like voltage and is explained from the flux decay theorem. Further explanation is, delay is due to inertial time lag $\tau_s = \frac{L_s}{R_s}$ effecting the rotor induced electromotive force (emf) V_{0r}. The flux during fault is given by

$$\Phi_{sf}^s = \Phi_s^s e^{-t/\tau_s} \tag{8}$$

and $\frac{d\Phi_{sf}^s}{dt}$ is negative, indicating its decay. By substituting (8) in (1b)

$$V_{0r}^s = \frac{L_m}{L_s}\left(-\frac{1}{\tau_s} + j\omega e^{-t/\tau_s}\Phi_s^s\right) \tag{9}$$

The above equation is converted into a rotor reference frame and neglecting $\frac{1}{\tau_s}$

$$V_{0r}^s = \frac{L_m}{L_s}(j\omega)\Phi_s^s e^{-j}\omega t \tag{10}$$

By substituting $\Phi_s^s = \frac{V_s^s}{j\omega_s} e^{j\,\omega_s t}$ in (10)

$$V_{0r}^r = -\frac{L_m}{L_s}(1-s)V_s e^{-jt(\omega-\omega_s)} \tag{11}$$

$|V_{0r}^r|$ is proportional to (1−s)

The converting equation (1a) into the rotor reference frame

$$V_r^r = V_{0r}^r e^{-j}\omega t + R_r i_r^r + \sigma L_r \frac{di_r^r}{dt} \tag{12}$$

A substantial decrease in pre-fault voltage at steady state V_{0r}^{r} to a particular voltage during a three phase fault was explained from the above analytics. Though, RSC converter is intended to meet V_{r}^{r} to match V_{0r}^{r} for rotor current control and the design of converters is for rating of only 35% of stator nominal voltage. The voltage dip during fault is controlled independently or in coordination using two techniques is explained as follows.

During fault, at first instant, the stator flux (Φ_s) does not fall instantly given by Eq. (8). The DFIG rotor speed is assumed to be running at super synchronous speed with slip (s) around −0.2pu at steady state. During fault, rotor speed advances to more speed based on the term (1−s) given by (11). The above speed variation is uncontrollable for a generator like DFIG which has higher mechanical and electrical inertia constants. This makes large inrush currents entering into the stator and rotor windings. To control the rotor current change in faults, the V_{r}^{r} value must be increased accordingly.

From the first technique as explained above, a voltage $V_{\Phi s}$ needs to be injected into the feed forward path to compensating the rotor voltage dip to regain to its steady state value of fault or immediately once fault is relieved. Converting the Eq. (7) into a synchronous reference frame and in view of direct alignment of Φ_{ds} with $\Phi_s$we get,

$$V_{\Phi s} = -\frac{L_m}{L_s}\omega\Phi_{ds} \tag{13}$$

The second technique for rotor voltage increase necessity is, this dip can be compensated by replacing $s\omega_s$ with $(\omega_{\Phi s} - \omega)$ in the cross coupling components terms $s\,\omega_s L_r' i_{qr}$ and $s\omega_s L_r' i_{dr}$ respectively. The reduction in magnitude and frequency of stator flux Φ_s, and configuration of flux with the stator voltage without considerable variations in the rate of change in flux angle $\theta_{\Phi s}$ specifies dc offset component in flux given by Eq. (14a).

$$\frac{d\theta_{\Phi s}}{dt} = \omega_{\phi s} = 0 = \omega_f \tag{14a}$$

Here, ω_f is the speed of stator flux during fault and this value can be made to zero as offset.

The voltage injection terms in Eqs. (12), (13) and compensating components terms in Eq. (14a) as discussed are anticipated using enhanced flux oriented control (EFOC) scheme for RSC circuit is shown in Fig. 2 and the determined values are incorporated in the RSC controller.

$$\frac{d\Theta_{\phi s}}{dt} = \omega_{\phi s} = \frac{V_{\beta s}\phi_{\alpha s} - V_{\alpha s}\phi_{\beta s}}{\phi_{\alpha s}^2 + \phi_{\beta s}^2} = \omega_f \tag{14b}$$

For better dynamic stability of grid connected DFIG, proposed method controls the decrease in the stator and rotor flux magnitude with control in decay in flux decomposition and damps power and torque oscillations during fault instances. To get better operation during disturbances, this paper adopts a strategy for rotor frequency reference to change from zero or other smaller value depending on the type and severity of the disturbance. This makes the phase locked loop of RSC to change its value of the fault, which makes the synchronization to stator voltage accordingly. This reduces the flux decay in stator and rotor windings effectively during faults. This ensures the dc offset components entering into the DFIG windings. Hence overall performance of grid connected DFIG is technically improved. The precise measurement of stator and rotor parameters like flux, voltage, speed, angle and current helps in achieving better performance during disturbances. The reduction in dc offset stator current at transients and getting the two axis flux and voltage trajectories circular will improve the efficacy of the DFIG system during any faults. The Eqs. (4)–(8) helps to understand the grid connected DFIG behavior during transient conditions and accuracy of its working depends on measurement of rotor current and flux parameters.

The grid side controller (GSC) circuit block diagram is shown in Fig. 1 and RSC for enhancing performance for LVRT issues is shown in Fig. 2. During normal conditions, the reactive power will be zero or very low and hence stator power pumped to grid will be high. This power control can do use the outer control loop of GSC. The reference power is obtained from the characteristic lookup table based on the DFIG adopted. This reference power is compared to actual power and is maintained using the PI control of GSC as shown in Fig. 1. During faults, the reference stator power changes based on the reactive power demand, which will be supplied by GSC through the capacitor at the back to back converters. As reactive power demand increases, stator power changes accordingly, and hence the terminal voltage at GSC change respectively and thereby direct axis current injecting at the point of common coupling (PCC) changes. Similarly, during normal conditions, stator rms voltage is constant and also reactive power will remain constant. But when fault occurs, the stator voltage changes, hence reference rms stator voltage changes. This will make the quadrature component of GSC current to vary. This total mechanism is fast and can work for symmetrical as well as asymmetrical faults.

$$E_{dR} = \frac{-L_m}{L_s}(V_{qS} + \lambda_{dR}\omega_r) \text{and} E_{qR} = \frac{L_m}{L_s}V_{qS}$$

For particular wind speed, reference or optimal mechanical power from the turbine is estimated using a characteristic lookup table. In detail, the stator real power (P_{stator}) is measured and power error is the difference between these two powers (dP) which have to be maintained to zero using a PI controller. The PI output is then multiplied to the real power constant (K_p) gives actual power to be controlled after disturbance. The change in the square of the reference capacitor voltage DC link (V_{dc}^{*}) and square of actual capacitor voltage (V_{dc}) is controlled by the PI controller of reference controllable real power. The change in reference to actual controllable power is divided between $2/3V_{sd}$ to get d-axis current near grid terminal (I_{gdref}). Change in I_{gdref}^{*} and actual grid current I_{gdref} is controlled by PI to get d-axis voltage. For a better response during transient state, decoupled d-axis voltage is added as doing for separately excited DC motor control methodology. The decoupling helps in improving steady state error and tie up the transient response of DFIG during LVRT or when sudden real or reactive power changes to or from the system.

In the same way generally stator voltage ($V_s^{*} = 1$) or reference reactive power ($Q_s^{*} = 0$), actual stator voltage Vs or reactive power Q_s is decreased by the PI controller and multiplied with the reactive power constant (K_q) for actual reference reactive power recompense parameter. The actual reactive power is designed and this difference and actual reactive power compensating terms and dividing with $2/3V_{sq}$, to get q-axis reference current (I_{qref}). The difference in I_{qref} and I_q is controlled using PI to get reference q-axis voltage. To improve the transient response quickly and to minimize steady state error decoupled q-axis voltage to be added. Both d and q axis voltage so obtained are converted to three axis 'abc' parameters with inverse Park's transformation and this voltage is given to the PWM controller for grid side controller pulse generation.

With the changes in wind speed, rotor speed will also change by shifting the gears position in the wind turbine. If rotor speed is made to operate on reference wind speed, maximum power can be extracted from wind turbine generator set. This will happen to normal state of operation, but during abnormal conditions like faults, rotor speed increases which may damage gears of wind turbine. Hence speed of DFIG rotor must be controlled. As explained in Section 2A, if the RSC is operated, the performance of DFIG can be

improved. With deviation in rotor speed, direct axis current of RSC changes and with demand in reactive power during faults or so, quadrature axis component of current changes. When a fault occurs, speed of rotor changes and hence rotor frequency also changes. If with this changed rotor frequency, current is injected into the windings of stator terminal of DFIG, flux decay or oscillations in stator terminal can be reduced. This will further to reduce the dc offset components of stator as explained from Eqs. (8)–(14b).

3. Control scheme for super capacitor to overcome LVRT for grid connected DFIG

The general layout of DFIG grid connected system is shown in Fig. 4. The design topology of UCESS system is shown in Fig. 3a [21] with different approach for the control strategy. Thevenin's model is used to describe the energy storage in the capacitor. The values of the UCESS parameters are given in the Appendix. The super capacitor consists of multiple numbers of cells in series (n_s) and in parallel (n_p) to achieve desired voltage (E_s) and current (I_{sc}) during normal and during the fault current control operation. The equations for SCESS are given below. The maximum rated voltage for SCESS is given by the product of number of series cells and voltage across each cell (V_{cell}). The total resistance drops across the series cells is given by product of series cells and resistance of each cell. The number of parallel cells gives the desired current given by the relation between max desired super capacitor (SC) current (I_{sc_max}) and current rating of each individual cell (I_{cell}). The maximum SC current can be estimated at SC power rating (P_{sc}) and maximum achievable SC voltage (V_{sc_max}). The total resistance of SC cells can be obtained from series resistance and parallel combination of cells. The total voltage output from SC is given by the product of total combination of half of the series cell capacitance and square of the voltage across SC. The capacitance required for SC during steady state is given by relation between SC power (P_{sc}) and maximum and minimum rating of SC voltage. The same capacitance required during low voltage fault ride through is given by Psc, rated SC value, energy stored in the capacitor (EST) and time up to which compensation is to be made.

$$\begin{cases} V_{sc\_max} = n_s * V_{cell} \\ R_s = n_s * R_{cell} \\ C_s = \frac{C_{cell}}{n_s} \\ n_p = \frac{I_{sc\_max}}{I_{cell}} \\ I_{sc\_max} = \frac{P_{sc}}{V_{sc\_max}} \\ R_{sc} = \frac{R_s}{n_p} \\ E_s = \frac{1}{2} C_{sc} * V_{sc}^2 \\ C_{scESS} = \frac{2P_{sc}t_d}{(V_{sc\_max} - V_{sc\_min})^2} \\ C_{SCESS} = \frac{2P_{sc}\Delta t_{LVRT}}{Est * V_{sc\_rated}^2} \end{cases} \quad (15)$$

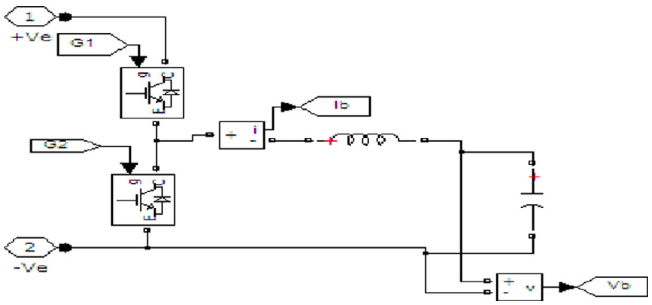

Fig. 3a. Connection diagram of SCESS at the back to back connection of DFIG converters.

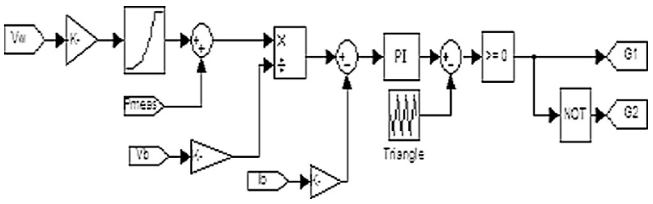

Fig. 3b. Control strategy of SCESS to compensate for voltage mitigations during faults and also for solving penetration issues.

The chopper circuit of SCESS is shown in Fig. 3a. Two IGBTs, an inductor and a high capacitance rating capacitor is used. Voltage and current sensors are used for measuring and for inputs to control circuit. Compared to battery, capacitors are faster in action, more reliable with no maintenance and long life. However initial cost of super-capacitor is high. The two IGBTs with anti-parallel diode based chopper circuit act as bi-directional current with constant polarity voltage source. This circuit acts as buck-boost based on grid- GSC voltage potential. Under normal conditions, the capacitor is charged and abnormal conditions like voltage sag at grid, the capacitor discharges to give desired reactive power respectively.

The control strategy for SCESS chopper circuit is shown in Fig. 3b. Here under normal conditions without grid disturbances, based on wind speed, desired power is estimated using the lookup table. The difference in the reference and measured actual real power is compared and the result is divided between SCESS voltage to get desired current flows from/to the SC. Note that, in this circuit diagram, the stator power is considered negative with respect to mechanical power. Hence, measured power is added to reference power. The difference in the reference and actual current measurement is controlled using a tuned PI controller. The voltage reference output from PI controller is compared with a triangular or saw tooth waveform to get pulses of the IGBTs. The overall control action is fast and accurate. To find the efficacy of the chopper circuit as external energy sources and EFOC technique for LVRT symmetrical and asymmetrical faults, simulation studies are done.

4. Simulation result and discussion

The DFIG grid connected system under study is shown in Fig. 4. The grid and rotor side converters are shown in Figs. 1 and 2. The doubly-fed induction generator is driven by a wind turbine. As per the RSC design, based on wind speed, rotor speed changes during normal conditions. Under low voltage fault conditions, generally rotor speed increases rapidly. With proposed EFOC technique, the rotor speed is controlled by the inner control loop of RSC. It is done by changing the reference speed of rotor position in a small value based on fault conditions. During this process, the rotor and stator

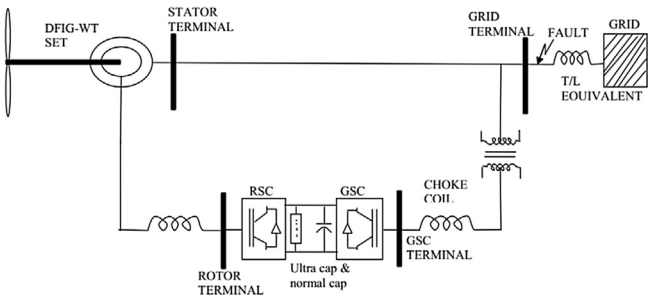

Fig. 4. Grid connected DFIG with ultra capacitor and normal capacitor configuration.

flux decays oscillations are controlled using this improved demagnetization control. A rapid and accurate control of reactive power by GSC and stator voltage and current control also helps the DFIG to have better performance during faults compared to the literature.

The performance of grid connected DFIG with proposed control circuits of a standard system shown in Fig. 4 is analyzed and compared with the works in the literature [27,28]. The system is analyzed for three cases. First case is single line to ground (SLG) fault with fault in A-phase. In the remaining two cases, double line to ground (DLG) and triple line to ground (TLG) is considered. In all the three cases, the fault is assumed to occur at point of common coupling (PCC) near the grid terminal with fault resistance of 0.001 Ω. The parameters of DFIG, converters, super or ultra capacitor rating etc are given in the Appendix.

4.1. Case A: SLG fault

A single line to ground (SLG) fault is assumed to occur to PCC during 0.1 to 0.3 s with phase A grounded with fault resistance of 0.001 ohms and the DFIG parameters are shown in Fig. 5. In the Fig. 5a, the results are taken from reference [28], Fig. 5b with [27] and Fig. 5c is our proposed EFOC technique. The fault assumed to occur at PCC near grid and as stator of DFIG is directly connected to grid, the stator voltage is decreased to nearly 90% of nominal value of 1pu (per-unit). In all three sub-figures stator voltage is almost same before, during and after the fault. The stator and rotor current during normal conditions is 1pu. Compared to Fig. 5a and b, the stator current in Fig 5c is almost constant. The current surge at the fault instant is less than 2 pu without any oscillations. Similarly, the rotor current is also almost constant without much change in magnitude or frequency in the waveform. During and after the fault behavior improvement of DFIG is possible with coordinated control of RSC and GSC with fast acting EFOC technique. The reactive power injection is done from both GSC and RSC and voltage profile improvement with quadrature component current control. Flux decay and oscillations control during and after the fault with offset DC component control scheme helps in achieving the performance. The electromagnetic torque (EMT) oscillations are also low and not reaching zero value during fault. The time for reaching its pre-fault value is quicker with our method as it is observed when the fault is cleared at 00.3 s. In Fig. 5a, the oscillations in the torque are damped quickly, but its magnitude is zero. However in Fig. 5b, it can be observed that the EMT oscillations are high.

The super-capacitor (SC) is placed in parallel with nominal rating capacitor at the back to back converters with control circuit as shown in Figs. 3a and 3b. The dc link voltage across the capacitor and also across the SC with base value of 400V is shown in Fig. 5 for a SLG fault. In Fig. 5a, dc link voltage fluctuating from 1 to 1.1 pu during fault and in Fig. 5b, the oscillations damped slowly but with peak value of 0.8 pu. With our proposed EFOC technique and with SC, the dc link voltage is almost constant during and after the fault. The voltage maintenance is not only with SC, but also with fast and accurate control of GSC and with SC chopper control scheme with enhanced current injection phenomenon.

The oscillations in both real and reactive powers in Fig. 5a and b during faults is more compared to our proposed technique. This can be achieved with fast acting GSC direct axis control scheme and external reactive power support from SC. The reactive power changed from −0.1 to +0.1 pu of reactive power during the fault. The real power has sustained oscillations during fault with value changing from 1 to 0.5 pu. Whereas with references [27,28], the oscillations are very high exceeding two to three times the nominal

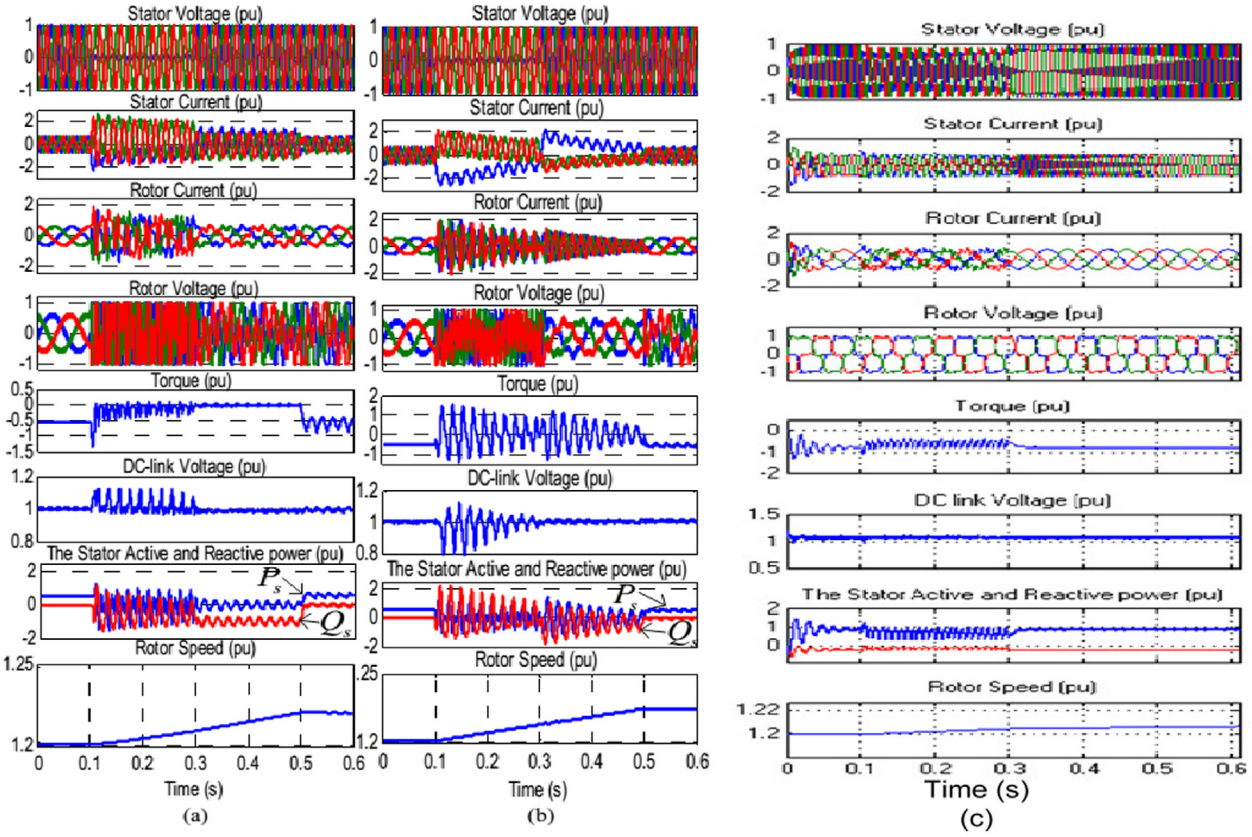

Fig. 5. The simulation results for a 90% single phase fault (a) The method in [28] (b) The method in [27] and right side figure (c) is our proposed method.

value. The rotor speed is almost constant with almost same speed of rotation during and pre-fault with our EFOC technique. With literature, the rotor speed changed to 1.23 from 1.2 pu during the fault. This is because of flux control scheme and rotor speed arbitrary reference change technique adopted in the paper. With this scheme, the rate of change of flux decay is controlled, by which the surge currents entering into the stator and rotor windings are controlled. The dc offset components with sub-transients are eliminated to a maximum extent during this most occurring SLG fault. The performance is greatly improved with EFOC technique when compared to the works in the literature.

4.2. Case B: DLG fault

In this case, another symmetrical fault called double lie to ground fault occurring between phase A and B with ground during 0.1 to 0.3 s at PCC is shown in Fig. 6. The results of our work are compared with [28] to observe the change in performance for same working environment with similar grid connected system under study. The fault is assumed to occur to phases A and B with ground at PCC near grid. In Fig. 6a, stator two voltages decreased to 0.3 pu from 1 pu and other healthy phase remained constant. For our system, two fault phases' stator voltages decreased to nearly 0.3 pu and other phase to 0.8pu for 1pu during the fault is shown in Fig. 5b. The stator current increased beyond 2 pu and nearly to 1.9 pu for the rotor during the fault can be observed from Fig. 6a. With proposed EFOC method, only at fault instant surge stator current reached 2 pu and decreased within a cycle and without any distortions in the waveform but with decreased magnitude to 0.8 pu from 1 pu in faulty phases. The healthy phase current remained almost constant. Similarly with EFOC, the rotor current is almost behaving same as stator current with surge current at fault instant reaching nearly 2 pu. There are some distortions in rotor current waveform but magnitude remained almost constant during the fault. The post-fault behavior with proposed scheme is very rapid than in the recently published paper [28]. This improvement in current performances is because of the fact of controlling dc offset components entering into the DFIG winding and control in flux decay.

The rotor voltage with proposed EFOC is almost constant with proposed technique as shown in Fig. 6b during and after the fault than with the output shown in Fig. 6a of [28]. The EMT behavior is almost same for both the methods, but damped very effectively with the work in [28] than our proposed system. However, the range of oscillations is from 0 to −0.5 pu for Fig. 6a, but with our proposed technique, it is from 0 to −0.3 pu. the post-fault recovery is very fast with our proposed system compared to Fig. 6a. The dc link voltage in Fig. 6a oscillates from 1 to 1.15 pu during fault and damped very quickly for [28]. With our proposed EFOC method, the dc voltage speed variation is from 1 pu to 0.5 pu. this value can be controlled and improved if SC capacitance is taken 0.02 F instead of 0.01 F.

The stator real power is having large oscillations from 0 to 1 pu and reactive from 1 to −1 pu for reference [28] as in Fig. 6a. With our scheme, the real power oscillates from 0 to 0.5 pu, but reactive power changed from −0.1 pu to 0.17 pu without oscillations with proposed EFOC technique during the fault as shown in Fig. 6b. the rotor speed is almost constant with small variation to 1.21 from 1.2 pu with EFOC in Fig. 6b, but the speed changed to 1.225 for work in [28]. The reason for the improvement holds equally good for SLG and DLG as explained in the previous case. They are, the decay in stator flux, arbitrary change in rotor frequency/speed reference frames, control in dc offset components of inrush current and large fluctuations in dc voltage across the capacitor. Hence our system performance holds good for DLG fault also. There is no need to calculate negative and zero sequence components

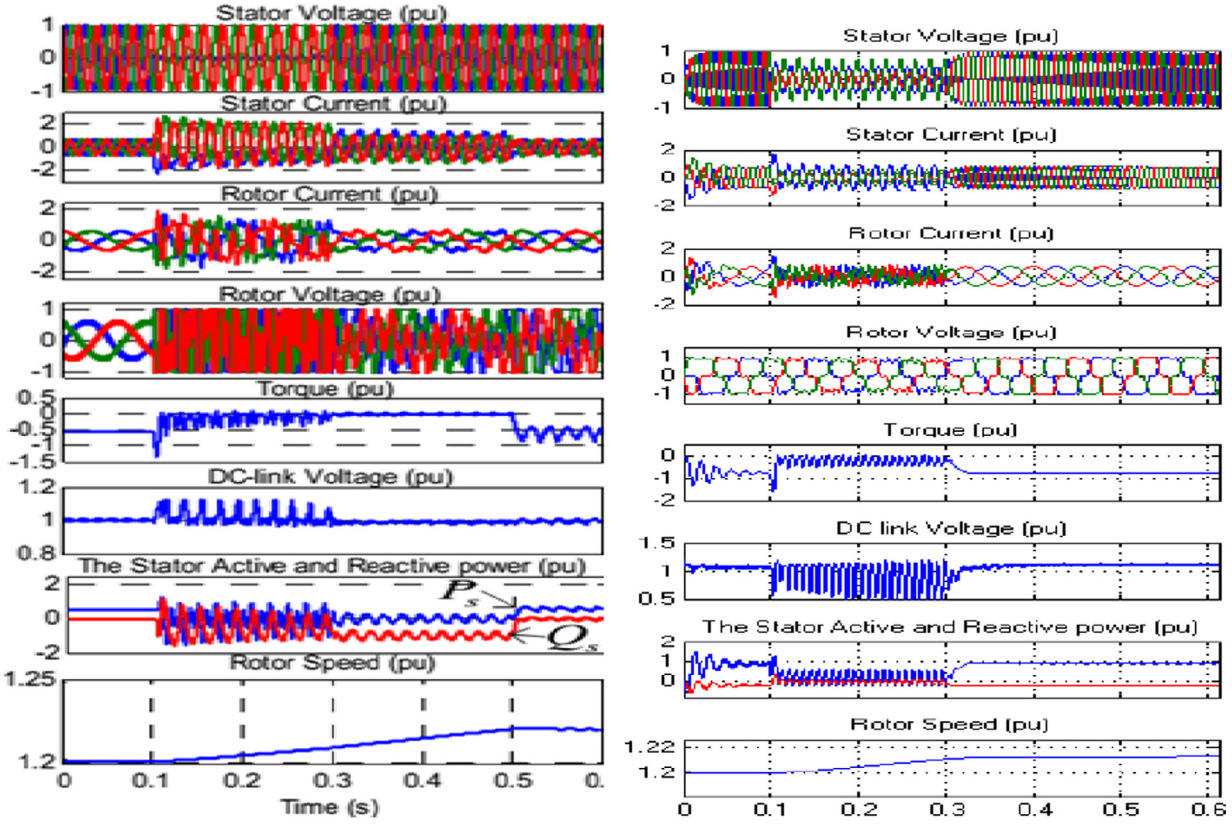

Fig. 6. The simulation results for a 70% double phase fault (a) The method in [28] (b) proposed EFOC method.

and control this with proposed EFOC technique. Therefore large complications in control circuit and mathematical analysis is eliminated.

4.3. Case C: TLG fault

In this case, three lines to ground (TLG) fault with 0.1 to 0.3 s occurring at PCC are considered and the results are shown in Fig. 7. The results from the literature [28] are shown in Fig. 7a is compared with results of our proposed technique in Fig. 7b. The stator three phase voltages decreased from 1pu to 0.3 pu during 0.1 to 0.3 s and the system is regained to normal once fault is cleared at 0.3 s. This dip is voltage in stator is due to fault which occurred near the grid. The stator is directly connected to grid for DFIG system and hence very much prone to grid disturbance. It is observed that, the rotor current which is 1 pu during the normal operation, the current increased to nearly 1.8 pu with distortions in the waveform with dc components as in Fig. 7a. The surge in the rotor current at fault instant reached 1.8 pu and immediately settled to 0.3 pu till the fault is cleared.

Once the fault is cleared, the current in the rotor is restored to normal in much less than a cycle time. The part of fault inrush current is allowed to pass through the DFIG windings and the remaining inrush current is allowed through the GSC converter and is stored in the capacitor and super-capacitor. Because of fast acting GSC, the current is returned to the grid through the IGBT converters of GSC. The current absorption by GSC depend on the converter rating, capacitor storage, reactive power supply requirement by

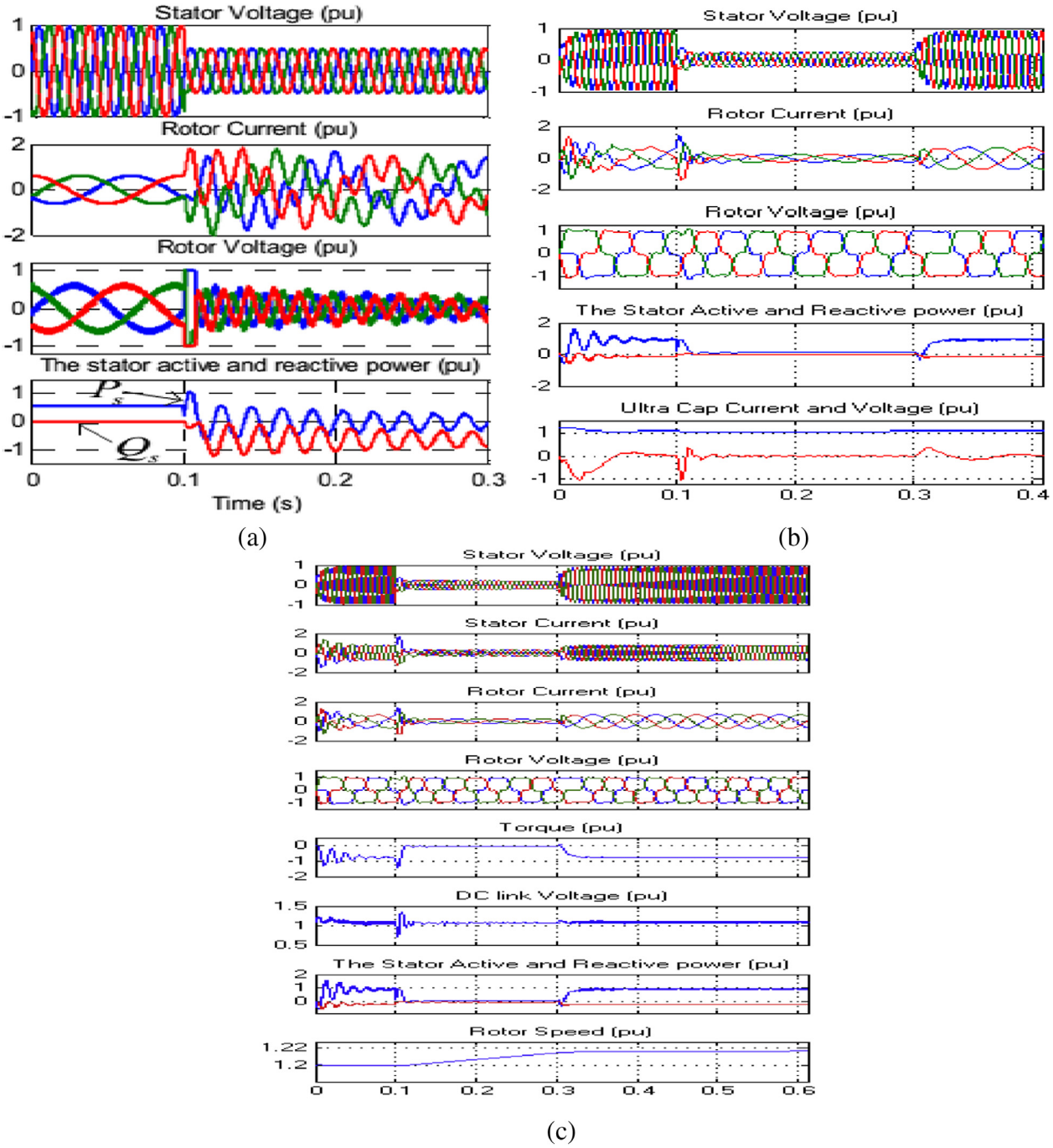

Fig. 7. The simulation results for a 70% three phases fault (a) The method in [28] (b) our proposed system. (c) detailed waveforms for TLG fault with proposed technique.

grid and fast acting control strategy. In our case, capacitor storage is high as SC is used and GSC action is fast and accurate. This logic helps in controlling inrush currents entering the DFIG windings and also makes system continues to operate effectively in fault but with small decrease in performance.

The rotor voltage decreased in magnitude, has change in frequency and has distortions in the waveform for [28] as in Fig. 7a, but is constant for the proposed system in Fig. 7b. It is due to the fact that the dc link voltage across the capacitor is nearly constant. It is maintained nearly constant because of fast acting GSC control scheme and capacitor rating is high. The stator active powers in Fig. 7a with oscillations decreased to zero average value and in Fig. 7b decreased from the nominal value to 0.15 pu during the fault. With our proposed scheme, there are no oscillations in the real power. The reactive power has oscillations from 0 pu to −1 pu during the fault with control in [28], whereas with our scheme, the reactive power without oscillations changed from −0.05 pu to 0.1 pu during the fault. Once fault is cleared, the real and reactive stator powers regained to normal value. The voltage and current waveforms of super-capacitor (SC) are shown in Fig. 7b. The voltage is nearly constant at 1.05 pu (with base 400 V, actual 415 V). The dc current through the super-capacitor is changing its value of the fault occurring and relieving instants with different injections and polarity values.

The detailed waveforms with stator current, electromagnetic torque and rotor speed with proposed control scheme are shown in Fig. 7c. It is observed that stator current surge is observed at fault instant and cleared immediately. In this, the inrush currents are controlled, thereby stator current rapid increase and fluctuations are limited. Also dc components produced by sub-transient and transient components of currents are also limited and thereby stator current waveform is nearly sinusoidal during the fault period. The electromagnetic torque naturally reached zero during the fault without any oscillations. The dc link voltage across the capacitor is having small surges at fault instant as there is a sudden change in grid terminal voltage and inrush currents entering into the GSC. In the earlier Fig. 7b, the voltage is across super-capacitor and a chopper circuit is present. Therefore, these two voltages are not similar even though they are in parallel between the dc terminals. The rotor speed is also nearly constant at 1.2 pu during and pre-fault with small deviation of 0.02 pu.

The proposed EFOC control scheme works effectively for symmetrical faults also. There are no power oscillations, torque pulsation, no rapid change in speed and stator and rotor currents are also sinusoidal without much change in its voltage magnitude and frequency. The same working law for asymmetrical faults holds good for symmetrical faults without any necessity to measure negative and zero sequence components. Hence, proposed control circuit design is simple and robust with effective working for any type of fault and with large dip in the grid voltage. GSC helps in maintaining constant dc voltage across capacitor. The super-capacitor helps in supplying desired reactive power to the grid to overcome the severe inrush currents entering into the DFIG windings. The RSC control scheme helps in maintaining rotor speed constant by decaying the flux in stator and rotor during the faults. Also, the direct and quadrature axis current control scheme, thereby voltage references to PWM are quick enough to adopt for any type of fault with severity. Hence proposed scheme is very efficient in operating during and after fault with good stability margin.

5. Conclusion

The wind energy conversion system (WECS) with good LVRT technique will ensure dynamic stability by complying with modern wind grid codes. A DFIG wind turbine system to limit transient over currents in rotor circuit is achieved by using proposed EFOC algorithmic technique. This is advanced demagnetization method of advances in the inner and external control circuit of RSc and GSC. Using proposed technique, application of crowbar circuit can be removed. A comparison is made with already existing simulation results from proposed method to show the efficacy of proposed control scheme. An external super-capacitor energy storage system (SCESS) is placed in parallel with a normal capacitor across the back to back converters for additional reactive power support. This method of DFIG system equally holds good for symmetrical as well as asymmetrical faults occurring at grid. With proposed technique, the overall dynamic response to the system is improved by suppressing not only fault transient but also post fault transients. This scheme improves the lethargic system to reach its steady state at an improved rate compared to the work in the literature. Thus, it provides good quality as well as reliable power with the aid of SCESS. Fast acting GSC controller can maintain dc voltage across capacitor nearly constant without ripples. It can further help in diverting fault inrush currents entering into the generator windings, hence protecting the DFIG without the use of external passive protective circuits like the crowbar etc. the RSC helps in controlling sub-transient dc off set currents entering into the rotor windings. It does by controlling the flux decay with appropriate change in reference rotor speed. By doing this, the phase locked loop (PLL) synchronizing with stator changes, which changes the current flow rate from/to the stator winding. Also faster control action of direct and quadrature rotor current also helps in compensating stator and rotor current waveforms. Hence overall performance is improved theoretically and analytically compared to the work in the literature.

In contrast, with work in literature, our method will control deviation in the dc link capacitor voltage with rotor speed is maintained constant and electromagnetic torque oscillations are damped effectively during and after the faults effectively. It is observed that when grid voltage dropped to 70%, the rotor voltage is still maintained constant during the fault with the aid of GSC and SCESS. The stator and rotor current waveforms preserved seamless during the fault with small change in its magnitude without much deviation from the operating natural frequency. The surge currents are also eliminated in less than a cycle time period. There is a dip in the generator winding currents during the fault and reached steady state immediately after the fault was cleared, thereby stability margin is improved. The capacitor voltage is also maintained nearly constant in magnitude during the fault. The ripples in EMT are reduced compared to the work in the literature. The overall system performance during the severe symmetrical and asymmetrical fault are improved using EFOC technique and further improvement is made with SCESS is incorporated in the DC link of the converters. The proposed method follows basic conventional law for grid connected DFIG with advanced performance compared to previous works.

Appendix

The parameters of DFIG used in simulation are:

Rated Power = 1.5 MW, Rated Voltage = 690 V, Stator Resistance Rs = 0.0049 pu, rotor Resistance Rr = 0.0049 pu, Stator Leakage Inductance Lls = 0.093 pu, Rotor Leakage inductance Llr1 = 0.1 pu, Inertia constant = 4.54 pu, Number of poles = 4, Mutual Inductance Lm = 3.39 pu, DC link Voltage = 415 V, Dc link capacitance = 0.02 F, Wind speed = 14 m/s.

Grid Voltage = 25 kV, Grid frequency = 60 Hz, Grid side Filter: Rfg = 0.3 Ω, Lfg = 0.6 nH, Rotor side filter: Rfr = 0.3 mΩ, Lfr = 0.6 nH, ultra- capacitor rating 0.001 F with 415 V with base voltage of 400 V is considered. Super capacitor Specifications:

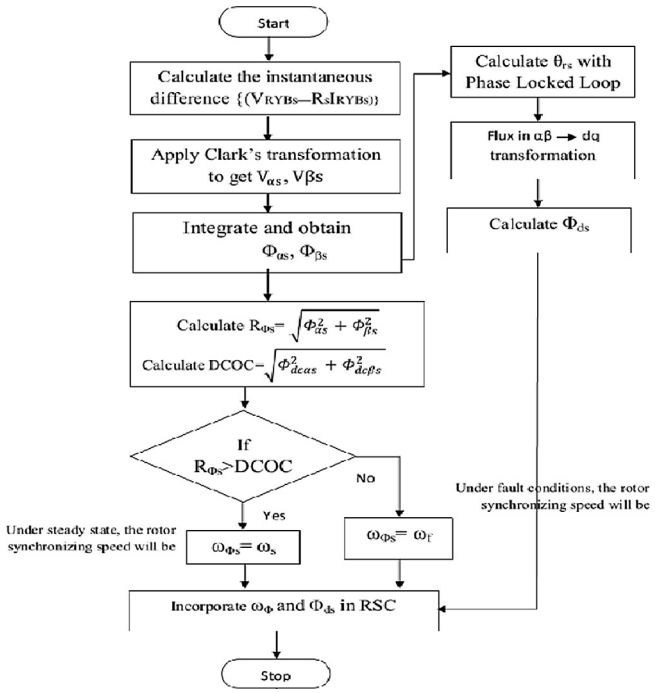

Fig. A1. Flowchart showing the procedure of EFOC method development in steps.

Cb = 180,000 uF, Rb = 10 kΩ, Rin = 0.2 Ω, Vocmax = 620 V, Vocmin = 500 V, Storage = 600 kW · h, L = 1 mH.

When dynamic stability has to be improved, proposed technique controls the decrease in stator and rotor flux magnitude and also damps oscillations at the fault instances. To achieve better performance during transients, this paper proposes a strategy for stator frequency reference to change to zero or other value depending type and severity of disturbance. The accurate measurement of stator and rotor parameters like flux, current helps in achieving better performance during transients. The DC offset stator current reduction during transients and making the two axis flux and voltage trajectories circular also improves the efficacy of the system performance during any faults. The Eqs. (8)–(12) help in understanding DFIG behavior during transient conditions and accuracy of its working depends on measurement of rotor current and flux parameters.

The Fig. A2 shows scheme of enhanced flux oriented control where, DCOC = DC offset component of flux, RΦs = radius of flux trajectory.

The voltage injection components (9), (10) and compensating components as discussed above are estimated using enhanced flux oriented control (EFOC scheme whose flow chart is shown here and

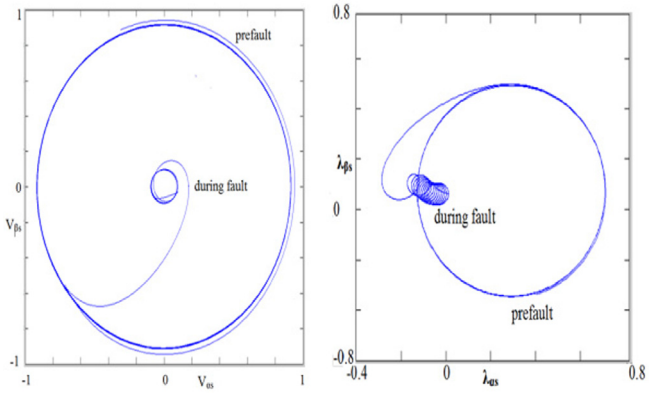

Fig. A3. Voltage and flux trajectories for a symmetric fault.

the determined values are incorporated in the RSC controller shown in Fig. 2.

In general the rotor speed is ω_r and the synchronous speed of stator, ω_s. But this synchronous frequency has to be changed from to a new synchronous speed value as described in flowchart ω_s' as it is represented commonly by $\omega_1 or \omega_f$. Under ideal conditions, reference stator d-axis flux Φ_d^* is zero and q-axis flux Φ_q^* is equal to the magnitude of stator flux Φ_s for given back emf and rotor speed. ω_s

The variation of stator and rotor flux trajectories before, during and after the fault is shown below in Fig. A3. The compensating components are estimated using enhanced flux oriented control (EFOC) scheme with a flow chart is shown in Fig. A1 and the determined values are incorporated in the RSC controller shown in Fig. 2.

The EFOC method of improving field flux oriented control technique helps in improving the performance of the RSC controller of DFIG during fault conditions is described in Fig. A1. The DCOC observer does two actions. The change in flux values of stationary frame stator references $(\Phi_{\alpha s}, \Phi_{\beta s})$ for tracking radius of the trajectory and the DCOC for offset change in stationary fluxes $(\Phi_{dc\alpha s}, \Phi_{dc\beta s})$ during fault conditions and controlling them is as shown in Fig. A3.

The first action helps in not losing the trajectory from a circle point, and to reach its pre-fault state with the same radius and centre of the circle and hence improving the same rate of flux compensation even during fault without losing stability. The second action helps in controlling and maintaining to nearly zero magnitude using the DCOC technique.

Based on above two actions, if former one is greater with change in trajectory which generally happens during disturbances from an external grid, stator synchronous frequency flux speed $(\omega_{\Phi s})$ changes to synchronous grid frequency flux (ω_s) otherwise

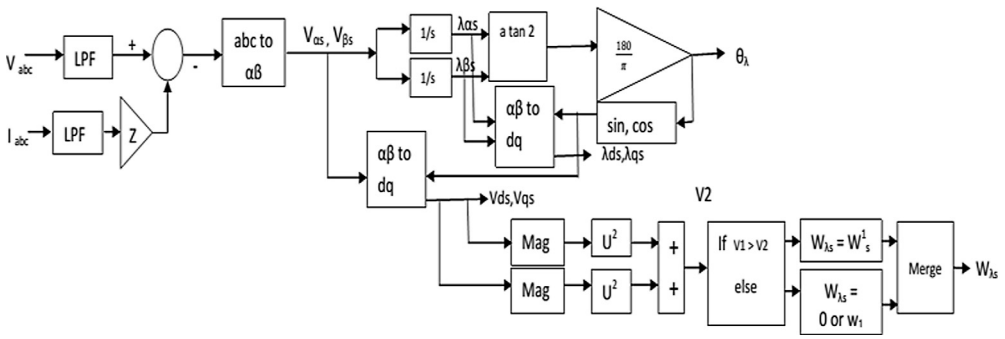

Fig. A2. EFOC control loop design with DCOC and rotor flux trajectory control.

$\omega_{\Phi s}$ changes to fault angular frequency value and is injected to RSC voltage control loop as error compensator.

The stator three phase voltages and current are used as inputs for extracting a new arbitrary reference frame for RSC during different fault levels. Here 'z' is the internal resistance of the stator winding. The voltage and current with impedance multiplication are subtracted to get reference voltage as shown in Fig. A2. Under normal conditions, the difference will be nearly zero. During fault conditions, the voltage decreases and current increases, which make the difference between these two parameters to the picture. Now the reference three phase voltages are converted to stationary alpha, beta ($V_{\alpha s}$, $V_{\beta s}$) voltages using Clark's transformation. This voltage is integrated and manipulated to get stator flux $\Phi_{\alpha s}$, $\Phi_{\beta s}$. The angle between these two fluxes is flux angle reference θ_λ. This angle is used to convert $\Phi_{\alpha s}$, $\Phi_{\beta s}$ to Φ_{ds}, Φ_{qs} and also the two stationary voltages $V_{\alpha s}$, $V_{\beta s}$ are also converted to rotating voltages V_{ds}, V_{qs} using parks transformation. The magnitude of these two voltages is V_2. The reference voltage magnitude of stator is V_1. During normal conditions, V_1 and V_2 are same. But during voltage dips, there exists a difference between the two voltages V_1 and V_2. During faults, if V_1 is greater than V_2, RSC inner control loop and speed reference changes from $W_{\lambda s}$ to W^1s. else in another case, with V_2 greater than V_1, the speed reference varies from $W_{\lambda s}$ to 0 or W_1. Under severe fault, where voltage dip will go beyond the rating of converters, the $W_{\lambda s}$ will be zero. Else it will have certain value specified by flowchart and controller as shown in Figs. A1 and A2.

References

[1] Yun Wang, Dong-li Zhao, Bin Zhao, Hong-hua Xu, A review of research status on LVRT technology in doubly-fed wind turbine generator system, in: Proc. on ICECE, 2010, pp. 4948–4953.

[2] Rongwu Zhu, Zhe Chen, Wu Xiaojie, Fujin Deng, Virtual damping flux-based LVRT control for DFIG-based wind turbine, IEEE Trans. Energy Convers. 30 (2) (2015) 714–725.

[3] Shuai Xiao, Geng Yang, Honglin Zhou, Hua Geng, An LVRT control strategy based on flux linkage tracking for DFIG-based WECS, in: IEEE Transactions on Industrial Electronics 60 (7) (2013) 2820–2832.

[4] Dong liang Xie, Zhao Xu, Lihui Yang, J. Ostergaard, Yusheng Xue, Kit Po Wong, A comprehensive LVRT control strategy for DFIG wind Turbines with enhanced reactive power support, in: IEEE Trans. Power Syst. 28 (2013) 3302–3310.

[5] Lihui Yang, Zhao Xu, J. Ostergaard, Zhao Dong Yang, Kit Po Wong, Advanced Control Strategy of DFIG Wind Turbines for Power System Fault Ride Through, in: IEEE Transactions on Power Systems 27 (2) (2012) 713–722.

[6] M. Rahimi, M. Parniani, Efficient control scheme of wind turbines with doubly fed induction generators for low-voltage ride-through capability enhancement, in: IET Renewable Power Gener. 4 (3) (2010) 242–252.

[7] Jiaqi Liang, D.F. Howard, J.A. Restrepo, R.G. Harley, Feedforward transient compensation control for dfig wind turbines during both balanced and unbalanced grid disturbances, in: IEEE Trans. Ind. Appl. 49 (3) (2013) 1452–1463.

[8] Jiaqi Liang, D.F. Howard, J.A. Restrepo, R.G. Harley, Feedforward transient compensation control for DFIG wind turbines during both balanced and unbalanced grid disturbances, in: IEEE Trans. Ind. Appl. 49 (3) (2013) 1452–1463.

[9] T.D. Vrionis, X.I. Koutiva, N.A. Vovos, A genetic algorithm-based low voltage ride-through control strategy for grid connected doubly fed induction wind generators, IEEE Trans. Power Syst. 29 (2014) 1325–1334.

[10] J.P. da Costa, H. Pinheiro, T. Degner, G. Arnold, Robust controller for DFIGs of grid-connected wind turbines, in: IEEE Trans. Ind. Electron. 58 (9) (2011) 4023–4038.

[11] J. Vidal, G. Abad, J. Arza, S. Aurtenechea, Single-phase DC crowbar topologies for low voltage ride through fulfillment of high-power doubly fed induction generator-based wind turbines, in: IEEE Trans. Energy Convers. 28 (3) (2013) 768–781.

[12] C. Abbey, G. Joos, Super-capacitor energy storage for wind energy applications, in: IEEE Trans. Ind. Appl. 43 (3) (2007) 769–776.

[13] W. Guo, L. Xiao, S. Dai, Y. Li, X. Xu, W. Zhou, L. Li, LVRT capability enhancement of DFIG with switch-type fault current limiter, in: IEEE Trans. Ind. Electron. 62 (1) (2015) 332–342.

[14] Wenyong Guo, Liye Xiao, Shaotao Dai, Enhancing low-voltage ride-through capability and smoothing output power of DFIG with a superconducting fault-current limiter-magnetic energy storage system, in: IEEE Trans. Energy Convers. 27 (2) (2012) 277–295.

[15] D.M. Yehia, Fault ride-through capability enhancement of DFIG-based wind turbine with supercapacitor energy storage, Power and Energy (PECon, in: 2014 IEEE International Conference on, Kuching, 2014, pp. 187–190.

[16] Q. Ling, Y. Lu, An integration of super capacitor storage research for improving low-voltage-ride-through in power grid with wind turbine, in: 2012 Asia-Pacific Power and Energy Engineering Conference, Shanghai, 2012, pp. 1–4.

[17] S. Divya, T. Krishna Kumari, Combination of super capacitor-switch type fault current limiter for LVRT enhancement of DFIG wind turbines, in: 2015 International Conference on Control Communication & Computing India (ICCC), Trivandrum, 2015, pp. 343–348.

[18] M.K. Döşoğlu, A. Basa Arsoy, U. Güvenç, Application of STATCOM-supercapacitor for low-voltage ride-through capability in DFIG-based wind farm, Neural Comput. Appl. (2016) 1–10.

[19] Raúl Sarrias-Mena, Luis M. Fernández-Ramírez, Carlos Andrés García-Vázquez, Francisco Jurado, Fuzzy logic based power management strategy of a multi-MW doubly-fed induction generator wind turbine with battery and ultracapacitor, Energy 70 (2014) 561–576.

[20] Spyros I. Gkavanoudis, Charis S. Demoulias, Fault ride-through capability of a DFIG in isolated grids employing DVR and supercapacitor energy storage, Int. J. Electr. Power Energy Syst. 68 (2015) 356–363.

[21] Irtaza M. Syed, Bala Venkatesh, Wu Bin, Alexandre B. Nassif, Two-layer control scheme for a supercapacitor energy storage system coupled to a Doubly fed induction generator, Electr. Power Syst. Res. 86 (2012) 76–83.

[22] Spyros I. Gkavanoudis, Charis S. Demoulias, A combined fault ride-through and power smoothing control method for full-converter wind turbines employing supercapacitor energy storage system, Electr. Power Syst. Res. 106 (2014) 62–72.

[23] A.H.M.A. Rahim, E.P. Nowicki, Supercapacitor energy storage system for fault ride-through of a DFIG wind generation system, Energy Convers. Manage. 59 (2012) 96–102.

[24] R.S. Weissbach, G.G. Karady, R.G. Farmer, A combined uninterruptible power supply and dynamic voltage compensator using a flywheel energy storage system, IEEE Trans. Power Delivery 16 (2001) 265–270.

[25] Cerezo A. Doria, Control and performance of a doubly-fed induction machine intended for a flywheel energy storage system, IEEE Trans. Power Electron. 28 (Jan 2013) 605–606.

[26] D.V.N. Ananth, G.V. Nagesh Kumar, Fault ride-through enhancement using an enhanced field oriented control technique for converters of grid connected DFIG and STATCOM for different types of faults, ISA Trans. 62 (2016) 2–18.

[27] D.W. Xiang, L. Ran, P.J. Tavner, S.C. Yang, Control of a doubly fed induction generator in a wind turbine during grid fault ride-through, IEEE Trans. Energy Convers. 21 (3) (Sep. 2006) 652–662.

[28] Shuai Xiao, Geng Yang, Honglin Zhou, Hua Geng, A LVRT control strategy based on flux linkage tracking for DFIG-based WECS, IEEE Trans. Ind. Electron. 60 (7) (July 2013) 2820–2832.

[29] S. Deepa, S. Rajapandian, Harmonic reduction technique using flying capacitor based Z source inverter for a DVR, in: Natl. J. Electron. Sci. Syst. 4 (1) (2013) 309–314.

[30] Max. Savio, S. Murugesan, Space vector control scheme of three level zsi applied to wind energy systems, Int. J. Eng. Trans. C Aspects 25 (4) (2012) 275–282.

[31] N. Sreeramulareddy, N. Senthil Kumar, Implementation of floating output interleaved input dc-dc boost converter, Int. J. Eng. Trans. C Aspects 28 (9) (2015) 1286.

[32] Navneet Kumar, Thanga Raj Chelliah, Satya Prakash Srivastava, Analysis of doubly-fed induction machine operating at motoring mode subjected to voltage sag, Eng. Sci. Technol. Int. J. 19 (3) (2016) 1117–1131.

[33] F. Harrou et al., A data-based technique for monitoring of wound rotor induction machines: A simulation study, Eng. Sci. Technol. Int. J. 19 (3) (2016) 1424–1435.

[34] Yuksel Oguz, Secil Varbak Nese, Mehmet Yumurtaci, Simulation and power flow control of wind-diesel hybrid power generation system, Technology 14 (3) (2011) 87–93.

[35] Babu, N. Ramesh, P. Arulmozhivarman, Wind energy conversion systems – a technical review, J. Eng. Sci. Technol. 8 (2013) 493–507.

[36] V. Nayanar et al., Wind-driven SEIG supplying DC microgrid through a single-stage power converter, Eng. Sci. Technol. Int. J. 19 (3) (2016) 1600–1607.